mL) was added, and the mixture was filtered. Hexane was added to the filtrate, and after shaking the organic layer was separated and dried over magnesium sulfate. The resulting solution was treated with bromine (6 g) in methylene chloride. Evaporation of the solvent left a white crystalline residue. Recrystallization from hexane gave styrene dibromide (4.7 g), mp 70.5-73.5 °C (lit.[25] 72-73 °C).

Propanal Dipropyl Acetal (4) from 1-Propanol. To a stirred mixture of pyridinium chlorochromate (48 g, 0.22 mol), Celite (15 g), and methylene chloride (200 mL) cooled in a water bath at room temperature (21 °C) was added 1-propanol (9.0 g, 0.15 mol). After 1.5 h, anhydrous ether (200 mL) was added, and the supernatant solution was decanted from the residual black gum. The black gum was extracted twice more with 100-mL portions of ether, and the combined organic phases were filtered through a column of Florisil. Anhydrous calcium chloride (60 g) and 1-propanol (30 mL) were added, and the mixture was left to stand for 24 h with occasional shaking. The mixture was filtered, and the filtrate was washed 5 times with dilute aqueous sodium bicarbonate. After drying over anhydrous sodium sulfate, the solvent was evaporated, and the residual oil was fractionally distilled under reduced pressure to yield pure compound **4** (3.2 g): ^{1}H NMR ($CDCl_3$) δ 0.92 (t, 3 H, J = 7 Hz, $CHCH_2CH_3$), 0.94 (t, 6 H, J = 7 Hz, $CH_2CH_2CH_3$), 1.60 (m, 6 H, CH_2CH_3), 3.46 (m, 4 H, OCH_2), 4.40 (t, 1 H, J = 6 Hz, OOCH).

***n*-Propylbenzene from 1-Phenyl-1-propyne.** A mixture of 1-phenyl-1-propyne (5 g), methanol (25 mL), and 5% palladium on carbon (0.2 g) was hydrogenated at 40 psi at room temperature for 12 h. The catalyst was filtered off, and the product *n*-propylbenzene (bp 159 °C) was isolated by distillation.

Acknowledgment. Partial support of this work was from Petroleum Research Fund Grant 17157-AC4, NIH Grant GM31801, and a gift from Alfred Bader, all of which are gratefully acknowledged. We thank James E. Jackson for several helpful discussions.

Registry No. :$C(CO_2Me)_2$, 15274-66-5; $C_6H_5(CH_2)_2Br$, 103-63-9; $Me(CH_2)_2OH$, 71-23-8; $C_6H_5C{\equiv}CMe$, 673-32-5; cyclohexane, 110-82-7.

(25) Fittig, R.; Erdmann, E. *Liebigs Ann. Chem* **1883**, *216*, 179-199.

Multiple-Quantum-Filtered Two-Dimensional Correlated NMR Spectroscopy of Proteins

Norbert Müller,[†,‡,§] Richard R. Ernst,[†] and Kurt Wüthrich*[‡]

Contribution from the Laboratorium für Physikalische Chemie, ETH-Zentrum, CH-8092 Zürich, Switzerland, and the Institut für Molekularbiologie und Biophysik, ETH-Hönggerberg, CH-8093 Zürich, Switzerland. *Received March 14, 1986*

Abstract: The use of multiple-quantum-filtered two-dimensional correlated spectroscopy (MQF-COSY) is investigated with regard to the identification of amino acid spin systems in proteins. In addition to a simplification of the spectra by the use of multiple-quantum filters, the multiplet structures and symmetry properties of the cross-peaks in MQF-COSY can give new information, which is complementary to that obtained from normal COSY. A catalogue of cross-peak patterns and cross-peak fine structures expected for the common amino acids is presented, and the practical consequences of modified selection rules for MQF-COSY with macromolecules are investigated. Optimized experimental procedures to minimize spectral artifacts and maximize sensitivity in MQF-COSY are described and applied to the protein basic pancreatic trypsin inhibitor (BPTI).

1. Introduction

Two-dimensional nuclear magnetic resonance spectroscopy (2D NMR[1])[2] is now an established tool for detailed structural studies of small proteins and DNA fragments.[3] Indentification of the individual ^{1}H-spin systems corresponding to the building blocks in these biopolymers is an important step in the spectral analysis. The first 2D experiments for structure determinations with proteins used absolute value displays.[4] In the meantime the power of 2D spectroscopy has been enhanced by recording pure phase spectra[5] and by two-quantum filtering.[6] These modifications improve the presentation of the 2D spectra with respect to multiplet resolution and phase properties without loss of relevant information. In spite of these advances it has become desirable to develop means for editing the complex ^{1}H NMR spectra of biological macromolecules into simpler subspectra. This can, for example, be achieved by selective excitation of certain spin systems[7] or by application of multiple-quantum filter techniques.[6,8,9] In contrast to 2D multiple-quantum spectra, where one frequency coordinate represents sums or differences of several chemical shift values, the representation of multiple-quantum filtered (MQF) COSY spectra does not differ from that of ordinary COSY. The spectra can therefore be analyzed with the same approach, and spectra obtained with p-quantum filters (pQF's) of different order p can be compared by simple superposition.

[†] Laboratorium für Physikalische Chemie.
[‡] Institut für Molekularbiologie und Biophysik.
[§] Current address: Institut für Chemie, Johannes Kepler Universität Linz, A-4040 Linz, Austria.

(1) Abbreviations used: 2D NMR, two-dimensional nuclear magnetic resonance spectroscopy; rf, radio frequency; FID, free induction decay; COSY, 2D correlated spectroscopy; MQF, multiple-quantum filter(ed); *p*QF, multiple-quantum filter of order *p*, with p = 2, 3, 4, ...; MQC, multiple-quantum coherence; *p*QC, multiple-quantum coherence of order *p*; BPTI, basic pancreatic trypsin inhibitor (Trasylol, Bayer AG, Leverkusen); TSP, trimethylsilylpropionic acid.

(2) Ernst, R. R.; Bodenhausen, G.; Wokaun, A. *Principles of Nuclear Magnetic Resonance in One and Two Dimensions*; Clarendon Press: Oxford, 1986.

(3) Wüthrich, K. *NMR of Proteins and Nucleic Acids*; Wiley: New York, 1986.

(4) (a) Nagayama, K.; Wüthrich, K.; Ernst, R. R. *Biochem. Biophys. Res. Commun.* **1979**, *90*, 305-311. (b) Nagayama, K.; Wüthrich, K. *Eur. J. Biochem.* **1981**, *114*, 365-374. (c) Wider, G.; Baumann, R.; Nagayama, K.; Ernst, R. R.; Wüthrich, K. *J. Magn. Reson.* **1982**, *42*, 73-78.

(5) (a) Aue, W. P.; Bartholdi, E.; Ernst, R. R. *J. Chem. Phys.* **1976**, *64*, 2229-2246. (b) Bachmann, P.; Aue, W. P.; Müller, L.; Ernst, R. R. *J. Magn. Reson.* **1977**, *28*, 29-39. (c) States, D. J.; Haberkorn, R. A.; Ruben, D. J. *J. Magn. Reson.* **1982**, *48*, 286-292. (d) Marion, D., Wüthrich, K. *Biochem. Biophys. Res. Commun.* **1983**, *113*, 967-974.

(6) (a) Piantini, U.; Sørensen, O. W.; Ernst, R. R. *J. Am. Chem. Soc.* **1982**, *104*, 6800-6801. (b) Shaka, A. J.; Freeman, R. *J. Magn. Reson.* **1983**, *51*, 169-173. (c) Rance, M.; Sørensen, O. W.; Bodenhausen, G.; Wagner, G.; Ernst, R. R.; Wüthrich, K. *Biochem. Biophys. Res. Commun.* **1983**, *117*, 479-485.

(7) (a) Levitt, M. H.; Ernst, R. R. *Molec. Phys.* **1983**, *50*, 1109-1124. (b) Levitt, M. H.; Ernst, R. R. *J. Chem. Phys.* **1985**, *83*, 3297-3310.

(8) Boyd, J.; Dobson, C. M.; Redfield, C. *FEBS Lett.* **1985**, *186*, 35-40.

0002-7863/86/1508-6482$01.50/0

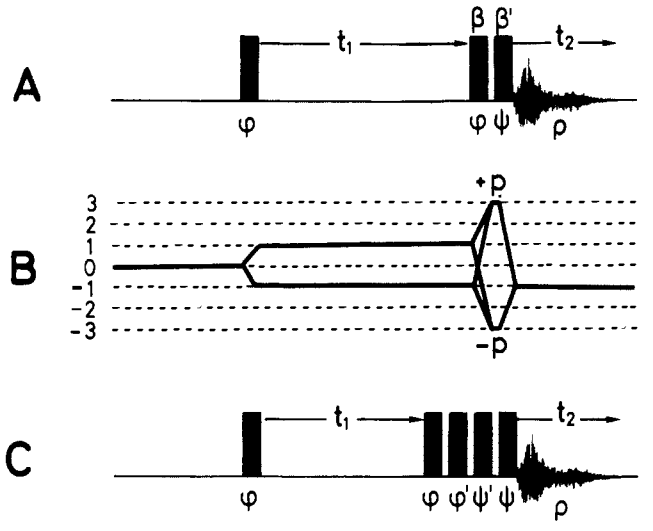

Figure 1. Experimental schemes for MQF-COSY: (A) Standard experiment as described in ref 6a. (B) Coherence transfer pathways for pure-phase pQF-COSY experiments. The numbers indicate the levels of coherence order.[13] In the spectral case considered here, $p = 3$. (C) Composite-pulse experiment designed to suppress flip angle artifacts which would reduce sensitivity. Normally all pulses are nominal $\pi/2$ pulses. Flip angle effects can be exploited by using $\beta,\beta' \neq \pi/2$. The phases $\varphi,\varphi'(=\varphi+\pi/2)$, $\psi,\psi'(=\psi+\pi/2)$, and ρ are varied in a phase cycle for the selection of the order p of the filter as given by eq 1 or 2.

Although the principle of multiple-quantum filtering has been known for some time, only few applications to biological macromolecules involving filters of an order higher than two have so far been reported.[8-10] This may in part be due to the high demands the methods impose on the instrumentation. In this paper we will be concerned with the MQF-COSY spectra of the amino acid spin systems in proteins. Special emphasis is on the multiplet structure of the cross-peaks, on signal intensities, and on potential artifacts. Effects of multiexponential relaxation[10] and of strong coupling will be discussed briefly in order to avoid pitfalls in the interpretation of the spectra. A more detailed report on these additional complications will be presented elsewhere.[11]

2. Principles of Multiple-Quantum Filtering

The basic MQF-COSY experiment was described by Piantini et al. al.[6a] and by Shaka and Freeman.[6b] It is based on the selection of multiple-quantum coherence (MQC) by combining experiments with phase-shifted pulse sequences.[12] In the following we present a brief survey of fundamental aspects of the method.

In p-quantum filtered COSY (Figure 1A) the first mixing pulse β following the evolution period t_1 generates p-quantum coherence (pQC) of all possible orders p. A second mixing pulse β' converts these coherences partially into observable -1 quantum coherence (-1QC). β and β' are usually $\pi/2$ rf pulses, as in all experiments in this paper. The desired multiple-quantum order p is selected by phase-cycling,[13] i.e., by coadding the results of $2p$ experiments with successively incremented phase ϕ of the first two pulses or of the phase ψ of the third pulse. The phase ρ of the receiver phase detector must be incremented at the same time according to

$$\varphi = n\pi/p,\ \rho = p\varphi,\ n = 0, 1, \cdots 2p-1 \quad \text{or} \quad (1)$$

$$\psi = n\pi/p,\ \rho = -(p-1)\psi,\ n = 0, 1, \cdots 2p-1 \quad (2)$$

respectively. A pQF-COSY experiment thus requires a phase cycle of $2p$ steps. Note that at the same time the orders kp, $k = \pm 1$, ± 3, ± 5, ... are also selected. Additional, independent phase cycling of the other pulses may be advantageous or even mandatory for the suppression of instrumental artifacts (see Section 7).

The relative sensitivity $S(p)$ of pQF-COSY spectra for n-spin systems with $n \geq p$ decreases roughly in powers of two for increasing order p.[14] This implies a need for extensive signal averaging for higher order pQF-COSY spectra. The phase cycles of increasing length for higher orders p (eq 1) can therefore easily be accommodated within the required total number of scans, particularly for samples with high demands on sensitivity, such as solutions of biological macromolecules.

The effects of multiple-quantum filtering on COSY spectra have previously been rationalized by the following coherence transfer selection rules:[6,14] (1) A diagonal peak in pQF-COSY spectrum can only appear when the "active" spin has resolved couplings to at least $(p-1)$ further spins. (The active spin is precessing during the evolution and detection periods.) (2) A pQF-COSY cross-peak between two resonances can only appear when the two active spins spins have $(p-2)$ additional common coupling partners with resolved couplings. (One of the active spins is precessing during evolution, the other during the detection period.)

These rules hold for weakly coupled spin systems. Additional peaks may become allowed for systems with magnetically equivalent spins and concomitant degenerate transitions, where effects of nonexponential relaxation become important,[10,11] and under the influence of strong coupling. The use and the limitations of these selection rules are illustrated in the following section with spectra of the amino acid residues which are commonly found in proteins.

3. Multiple-Quantum-Filtered COSY Spectra of the Common Amino Acid Residues

The schematic MQF-COSY spectra depicted in Figure 2 (parts A and B) can be derived in a straightforward manner from the MQF selection rules summarized in the previous section. For amino acid residues bearing methyl groups (Figure 2C) and for strongly coupled spin systems complicating features have to be considered (Section 6).

It can be seen from Figure 2 that the elimination of particular cross-peaks is characteristic of certain structural elements in the amino acid residues (individual diagonal peaks are usually not resolved in protein spectra and are therefore not useful for assignments). This information can be exploited to identify spin systems even without detailed analysis of the cross-peak fine structure.

A simple case of such spectral editing achievable with multiple-quantum filtering in protein spectra is the elimination of signals from the two-spin systems of glycine in ^2H_2O solution by 3QF-COSY (Figure 2A). Two examples can be found in Figure 3: the α proton resonances of Gly-12 and Gly-28 of BPTI are absent in 3QF-COSY, whereby both cross-peaks and diagonal peaks are fully suppressed. In the 3QF-COSY spectrum of Figure 3, this enables identification of the Pro-2 $\delta\delta$ cross-peak close to the diagonal, which is partially hidden by one of the diagonal peaks of Gly-28 in the 2QF-COSY spectrum.

The α and β protons in the amino acid residues Val, Ile, and Thr possess no common coupling partners, as long as the long-range couplings between the α proton and the γ proton can be neglected. This neglect is normally justified in the case of protein spectra, where these couplings are not resolved. The $\alpha\beta$ cross-peaks of the mentioned residues are therefore suppressed in 3QF-COSY according to the MQF selection rules (see Figure 2C). In Figure 4 this is exemplified by the elimination of the $\alpha\beta$ cross-peaks of Val-34 and Ile-18. It should be noted, however, that in these cases the diagonal peak of the β protons is preserved because of additional couplings to the γ protons.

Spectral editing by multiple-quantum filtering may be directly useful for the identification of the different spin systems, as well as for unravelling of spectral regions with mutually overlapping

(9) Rance, M.; Dalvit, C.; Wright, P. E. *Biochem. Biophys. Res. Commun.* **1985**, *131*, 1094-1102.
(10) Müller, N.; Bodenhausen, G.; Wüthrich, K.; Ernst, R. R. *J. Magn. Reson.* **1985**, *65*, 531-534.
(11) Müller, N.; Bodenhausen, G.; Ernst, R. R., submitted for publication.
(12) Wokaun, A.; Ernst, R. R. *Chem. Phys. Lett.* **1977**, *52*, 407-412.
(13) Bodenhausen, G.; Kogler, H.; Ernst, R. R. *J. Magn. Reson.* **1984**, *58*, 370-388.
(14) Sørensen, O. W. *Modern Pulse Techniques in Liquid State Nuclear Magnetic Resonance Spectroscopy*; ETH Dissertation, No. 7658, 1984.

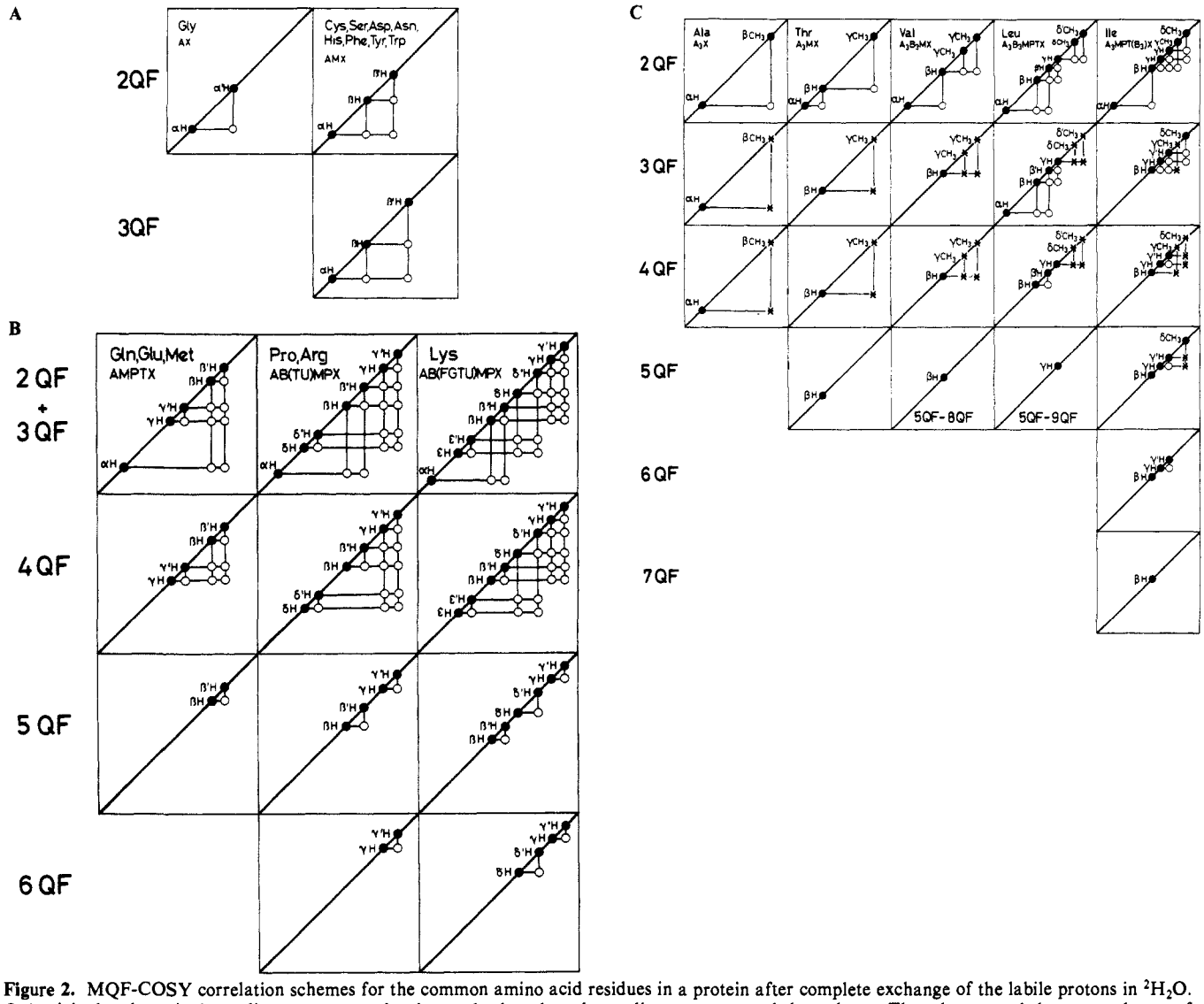

Figure 2. MQF-COSY correlation schemes for the common amino acid residues in a protein after complete exchange of the labile protons in ^2H_2O. Only vicinal and geminal couplings are assumed to be resolved, and weak coupling was supposed throughout. The schemes and the nomenclature of the proton spin systems are based on ref 3. Filled and open circles represent diagonal peaks and cross-peaks, respectively, that are predicted by the MQF selection rules. Asterisks mark the positions where "forbidden" cross-peaks may arise from multiexponential relaxation in methyl groups. (A) Spin systems that are fully suppressed by 3QF-COSY or 4QF-COSY, respectively. (B) Spin systems containing $(CH_2)_n$ fragments (n = 2, 3, 4). (C) Spin systems of the amino acid residues containing methyl groups. A–C contain all ^1H spin systems in the common amino acids except for those of the aromatic rings.

lines. Both the identification of spin systems and the analysis of crowded spectral regions can be further facilitated by exploiting the cross-peak multiplet structures, which are the subject of the following Section.

4. Multiplet Structures of MQF-COSY Cross-Peaks

The absorptive cross-peaks in phase-sensitive COSY and 2QF-COSY spectra contain as building blocks a square antiphase pattern that is duplicated for each passive spin I_k coupled to one or both of the two active spins I_1 and I_2 (Figure 5).[14,15] The antiphase structure is caused by the sine modulation of the signal under the influence of the coupling constant J_{12} between the active spins. The additional splittings in the ω_1 and ω_2 dimensions by the coupling constants J_{1k} and J_{2k} to passive spins acting during t_1 and t_2, respectively, lead to in-phase doublets, since they are caused by cosine modulation imposed by the couplings.

For an explanation of the cross-peaks in pQF-COSY spectra with $p > 2$ in an n-spin system with $n \geq p$, it is helpful to divide the spins into three classes: 1. The two *active* spins I_1 and I_2, which precess during t_1 and t_2, respectively, provide the center frequency coordinates Ω_1 and Ω_2 of the cross-peak and participate in the MQC. 2. The $(p-2)$ *MQ-active* spins I_k, which are involved in the intermediate pQC (Figure 1B), but are passive during t_1 and t_2. 3. The remaining $(n-p)$ *passive* spins I_l, which are not involved in any coherence but are coupled to one or both active spins I_1 and I_2.

The multiplet structure and the flip angle dependence of pQF-COSY spectra can be described by the following simple operator calculation. (Although these formula are necessary for the understanding of the pQF phenomena, they are not indispensable for an understanding of the following sections of this paper and may be skipped by a reader, who does not want to go too deeply into the fundamental aspects.) We will represent coherence by products of Cartesian angular momentum operators,[16] I_z, I_x, I_y, and shift operators,[18] I^+ and I^- (which are related to the Cartesian operators by $I^+ = I_x + iI_y$ and $I^- = I_x - iI_y$), for tracing out the pathways of the coherence transfer from spin I_1 during the evolution period, t_1, to spin I_2 during the detection period, t_2. The coherence transfer pathways[13] for pQF-COSY

(15) Neuhaus, D.; Wagner, G.; Vasák, M.; Kägi, J. H. R.; Wüthrich, K. *Eur. J. Biochem.* **1985**, *151*, 257–273.

(16) Sørensen, O. W.; Eich, G. W.; Levitt, M. H.; Bodenhausen, G.; Ernst, R. R. *Prog. Nucl. Magn. Reson. Spectrosc.* **1983**, *16*, 163–192.

(17) Sørensen, O. W.; Ernst, R. R. *J. Magn. Reson.* **1985**, *63*, 219–224.

(18) Abragam, A. *The Principles of Nuclear Magnetism*; Calderon Press: Oxford, 1961.

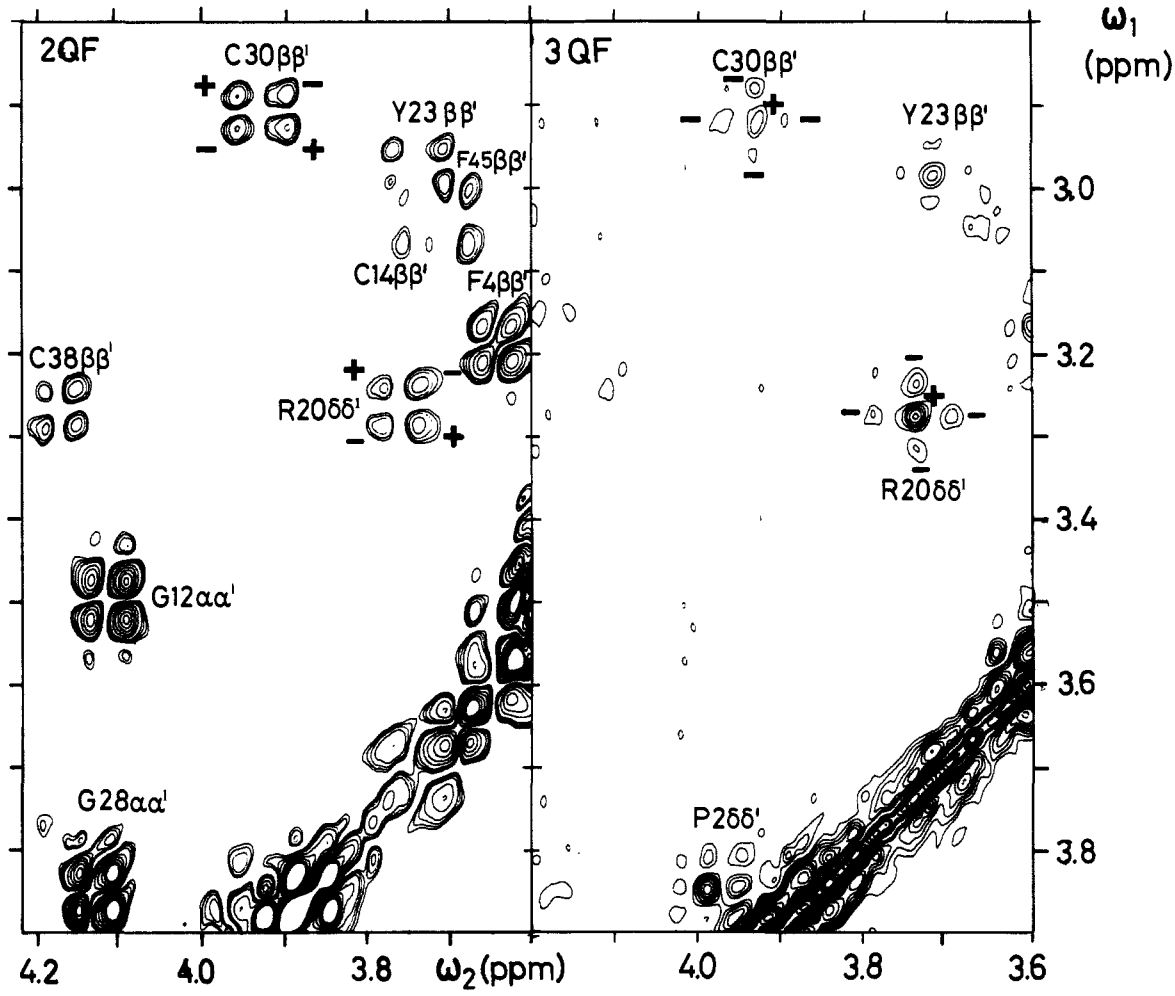

Figure 3. 2QF-COSY and 3QF-COSY of BPTI. A region containing geminal cross-peaks from Cys, Tyr, Phe, Gly, Arg, and Pro is shown. The cross-peaks are identified by one-letter symbols for the amino acid residues, their sequence position, and by the location of the protons in the side chain. While the sign pattern (indicated for Arg-20 $\delta\delta'$) in the 2QF-COSY cross-peaks is antisymmetric with respect to the chemical shift axes and there is zero intensity in the center, the 3QF-COSY cross-peaks have twofold symmetry with repect to both ω_1 and ω_2, there are intensity maxima in the centers. These maxima are positive in geminal cross-peaks if all vicinal coupling constants are positive, as in the case here.

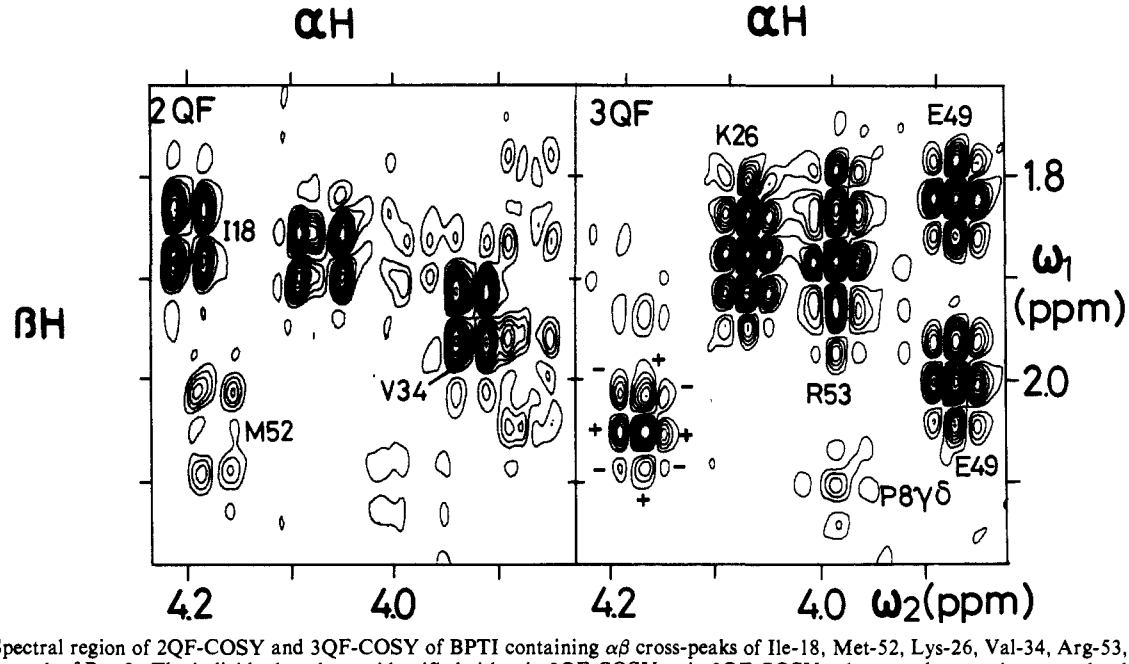

Figure 4. Spectral region of 2QF-COSY and 3QF-COSY of BPTI containing $\alpha\beta$ cross-peaks of Ile-18, Met-52, Lys-26, Val-34, Arg-53, Glu-49, and one $\gamma\delta$ cross-peak of Pro-8. The individual peaks are identified either in 2QF-COSY or in 3QF-COSY, wherever they can be more clearly recognized (see text).

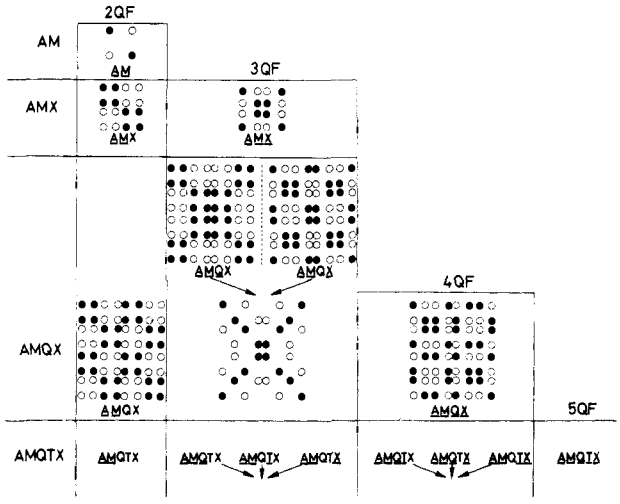

Figure 5. AM cross-peak multiplet patterns in weakly coupled nondegenerate 2-spin-, 3-spin-, and 4-spin systems in 2QF-COSY, 3QF-COSY, and 4QF-COSY. All coupling constants are assumed to be positive and different from each other. Filled and open circles indicate positive and negative intensities, respectively. The underlined letters denote those spins which participate in the pQC during the filter period. If the number of spins, n, exceeds the order p of the filter, several coherence transfer pathways are possible (eq 7). This may lead to cancellation of lines within the multiplets (see, e.g., in the 3QF-COSY cross-peak of the 4-spin-system). For the 5-spin system only the different pathways are indicated by designation of the MQC involved.

Table I[a]

$$f^+_1(t_1) = \sin(\pi J_{12}t_1)\prod_{k=3}^{p}\sin(\pi J_{1k}t_1)\prod_{l=p+1}^{n}\cos(\pi J_{1l}t_1)\exp(-i\Omega_1 t_1)$$

$$f^-_1(t_1) = \sin(\pi J_{12}t_1)\prod_{k=3}^{p}\sin(\pi J_{1k}t_1)\prod_{l=p+1}^{n}\cos(\pi J_{1l}t_1)\exp(+i\Omega_1 t_1)$$

$$f^-_2(t_2) = \sin(\pi J_{12}t_2)\prod_{k=3}^{p}\sin(\pi J_{2k}t_2)\prod_{l=p+1}^{n}\cos(\pi J_{2l}t_2)\exp(+i\Omega_2 t_2)$$

$$g^+(\beta) = \cos^2(\beta/2)\sin^{p-1}(\beta)$$

$$g^-(\beta) = \sin^2(\beta/2)\sin^{p-1}(\beta)$$

$$h^+(\beta') = \cos^2(\beta'/2)\sin^{p-1}(\beta')$$

$$h^-(\beta') = \sin^2(\beta'/2)\sin^{p-1}(\beta')$$

[a] Abbreviations used in eq 3–6 for the trigonometric coefficients of the spin operators. The symbols are explained in the text.

experiments are shown schematically in Figure 1B. During t_1, 1QC of spin I_1, created by the first rf pulse, precesses under the influence of the chemical shift and the scalar spin–spin interactions and yields the antiphase terms which are essential for the generation of the intermediate pQC

$$I_1^+ \xrightarrow{t_1} (-2i)^{p-1}I_1^+I_{2z}\prod_{k=3}^{p}I_{kz}f_1^+(t_1) \quad (3a)$$

$$I_1^- \xrightarrow{t_1} (2i)^{p-1}I_1^-I_{2z}\prod_{k=3}^{p}I_{kz}f_1^-(t_1) \quad (3b)$$

The trigonometric coefficients of the operator terms in eq 3–6 are represented by the functions given in Table I, and terms irrelevant for the process considered are neglected. When observing −1QC during the detection period, the I^+ operator terms existing during the t_1 period are responsible for the so-called N-peaks (or echo peaks), while the I^- terms give rise to the P-peaks (or antiecho peaks). In order to obtain a pure-phase spectrum, pathways with +1QC and −1QC during the evolution period are required at the same time.[5a] The proper antiphase terms are converted into $\pm p$QC by the first of the two mixing pulses, β (Figure 1A). The desired orders, $\pm p$, are selected by the choice of the phase cycling, leading to the transfers

$$(3a) \xrightarrow{\beta_y} (-i)^{p-1}[I_1^+I_2^+\prod_{k=3}^{p}I_k^+g^+(\beta) - I_1^-I_2^-\prod_{k=3}^{p}I_k^-g^-(\beta)]f_1^+(t_1) \quad (4a)$$

$$(3b) \xrightarrow{\beta_y} -(i)^{p-1}[I_1^+I_2^+\prod_{k=3}^{p}I_k^+g^-(\beta) - I_1^-I_2^-\prod_{k=3}^{p}I_k^-g(\beta)]f_1^-(t_1) \quad (4b)$$

The second mixing pulse, of flip angle β' (Figure 1A), converts $\pm qQC$ into antiphase −1QC of spin I_2

$$(-1)^p \times (4a) + (4b) \xrightarrow{\beta'_y} (-i)^{p-1}I_{1z}I_2^-\prod_{k=3}^{p}I_{kz}\{f_1^+(t_1)[g^+(\beta)h^-(\beta') + g^-(\beta)h^+(\beta')] + f_1^-(t_1)[g^+(\beta)h^+(\beta') + g^-(\beta)h^-(\beta')]\} \quad (5)$$

During the detection period the antiphase terms precess under the influence of the Hamiltonian accounting for chemical shift and spin–spin coupling and rephase according to

$$(5) \xrightarrow{t_2} \left(\frac{1}{2}\right)^{p-1}I_2^-\{f_1^+(t_1)[g^+(\beta)h^-(\beta') + g^-(\beta)h^+(\beta')] + f_1^-(t_1) \times [g^+(\beta)h^+(\beta') + g^-(\beta)h^-(\beta')]\}f_2^-(t_2) \quad (6)$$

Each of the sine terms in $f^+_1(t_1)$ and $f^-_1(t_1)$ produces an antiphase splitting in the ω_1 dimension, while the cosine terms in these functions lead to in-phase splittings. The term $f^-_2(t_2)$ has a corresponding effect on the multiplet structure in the ω_2 dimension. The sign pattern of the basic square is independent of the absolute sign of J_{12}, which is involved both in t_1- and t_2-precession. The sign patterns caused by the couplings to MQ-active spins I_k, however, depend on the sign of the products $J_{1k}J_{2k}$.[17]

By convention the spectra are phased such that the multiplet component in the upper left corner of all diagonal peak multiplets is positive. This is possible for all diagonal peaks irrespective of the signs of the coupling constants. The signs of the cross-peaks, however, represented by their left uppermost multiplet component, are determined by the signs of the products of all coupling constants causing a sine precession during t_1 or t_2. The couplings to passive spins not involved in the MQC cause an in-phase repetition of the complete antiphase pattern. In Figure 5 the basic multiplet patterns for 3QF-COSY and 4QF-COSY cross-peaks of nondegenerate 3- and 4-spin systems are drawn on the assumption that all coupling constants are positive but different in value. It is found that the sign patterns of the multiplets in odd-quantum-filtered COSY cross-peaks and diagonal peaks are symmetric with respect to the chemical shift axes, while even-quantum-filtered COSY cross-peaks are antisymmetric.

The multiplet structure in pQF-COSY spectra of n-spin systems with $p < n$ requires special attention. For example, in 3QF-COSY of a 4-spin AMQX spin system (Figure 5), two coherence transfer pathways contribute to an A-M cross-peak.[17] Both start at ±1QC of spin A during t_1 and end with −1QC of spin M during t_2, but one pathway passes through ±3QC of the three spins AMQ, while the other one involves ±3QC of the three spins AMX. The two pathways differ by the exchange of J_{AX} and J_{AQ} in causing sine and cosine modulation of the signal during t_1 and of the roles of J_{MX} and J_{MQ} during t_2. The superposition of these pathways leads to cancellation of half of the lines, as has been shown by Boyd et al.[20] This is the simplest manifestation of the general fact that application of a p-quantum filter with $p > 2$ to an n-spin system with $n > p$ results in a superposition of

$$m = \binom{n-2}{p-2} \quad (7)$$

contributions to the cross-peaks passing through p-spin p-quantum coherence, provided $\pi/2$ pulses are used. For even values of m this can lead to complete cancellation and for odd values of m to partial cancellation of certain multiplet components. For mixing pulses with $\beta,\beta' \neq \pi/2$, further pathways become allowed which are not relevant in the present context.

We should note that if the number of spins exceeds the order of the MQC, i.e., $n > p$, the intermediate pQC can also involve q spins with $q = p + 2, p + 4,...$ leading to q-spin pQC (e.g., 4-spin 2QC: $I_1^+I_2^+I_3^+I_4^-$). The multiplet structure of a q-spin contribution to a pQF COSY cross-peak is determined exclusively by the number q of spins involved in the coherence. Contributions for

$q > p$ are, however, often weak,[14] and cause only insignificant intensity distortions in MQF-COSY. In multiple-quantum spectra, on the other hand, these terms are responsible for well-separated combination peaks, which can easily be observed and are useful for assignments.[19] Here we restrict our attention to the dominant p-spin pQC.

5. Constructive and Destructive Interference of Cross-Peaks

In 2D NMR spectra of many macromolecules full resolution of the cross-peak fine structure is impossible because of the inherently large line width. The overall symmetry of the cross-peaks nevertheless often enables their identification. For example, in situations where adjacent peaks partially overlap, cancellation due to antiphase contributions may present difficulties in interpreting even-quantum-filtered spectra (in particular 2QF-COSY). In such cases application of an odd-quantum filter may be advantageous, since the symmetry of the cross-peaks with respect to the chemical shift axes makes cancellation less probable.

The different symmetry properties of peaks in odd- and even-quantum-filtered COSY spectra are illustrated in Figure 3. The striking difference between 2QF-COSY and 3QF-COSY (apart from the previously mentioned elimination of the Gly spin systems in 3QF-COSY) is that the 3QF cross-peaks have either positive or negative multiplet peaks near their centers (Figure 5), whereas even-quantum-filtered cross-peaks have zero intensity in the center. The sign of the central signal contribution in odd-quantum-filtered spectra recorded with low resolution (caused either by poor digitization or by large natural line widths) depends on the sign of the product of the coupling constants to the additional MQ-active spins. This can be exploited to distinguish between vicinal and geminal cross-peaks in low-resolution spectra, since all geminal proton–proton coupling constants in proteins are negative, and the vast majority of the vicinal couplings is positive. Consequently, the 3QF-COSY $\beta\beta'$ cross-peaks all have a positive center, as exemplified by Figure 3, since the passive vicinal $\alpha\beta$ coupling constants are of equal (positive) sign. Vicinal cross-peaks of $C^{\alpha}H$–$C^{\beta}H_2$ fragments in 3QF-COSY, on the other hand, usually have a negative center (Figure 4), as the coupling constants of the two active spins to the additional MQ-active spin are normally of opposite sign. Deviations from this rule would indicate negative vicinal coupling constants $^3J_{\alpha\beta}$, which could be of crucial interest for studies of polypeptide conformation.

When turning to the cross-peaks between the long side chain protons of the amino acids of Figure 2 (parts B and C), the situation is complicated by the fact that several contributions to the cross-peak multiplets may interfere (Figure 5). No general rules can be given here, but experimental evidence shows that the majority of the vicinal cross-peaks in 3QF-COSY have a negative center.

A further favorable feature of pQF-COSY with increasing order of p is the attenuation of diagonal peaks. This can be rationalized by the facts that the diagonal peaks for spins with less than $(p - 1)$ coupling partners are completely eliminated and that there are no dispersive contributions on the diagonal if an n-spin system is subjected to a p-quantum-filter with $p = n$ (there may be weak dispersive contributions, however, for $p < n$). This partial diagonal suppression, which is readily appreciated by the reduction of its apparent width in the contour plots, is of considerable advantage for localizing cross-peaks between spins with similar chemical shifts, as is exemplified in Figure 3.

The attenuation of peaks due to cancellation of antiphase pairs of multiplet components in COSY and 2QF-COSY may pose serious problems in spectra with broad lines.[15] Figure 5 shows that for higher order MQF-COSY spectra, in-phase pairs of multiplet components occur in the interior of the cross-peaks. For odd-order pQF-COSY cross-peaks ($p \geq 3$) there are at least four multiplet components of equal sign arranged near the multiplet center, while in even-order MQF-COSY spectra the antisymmetric multiplets have a zero integral also over the central components.

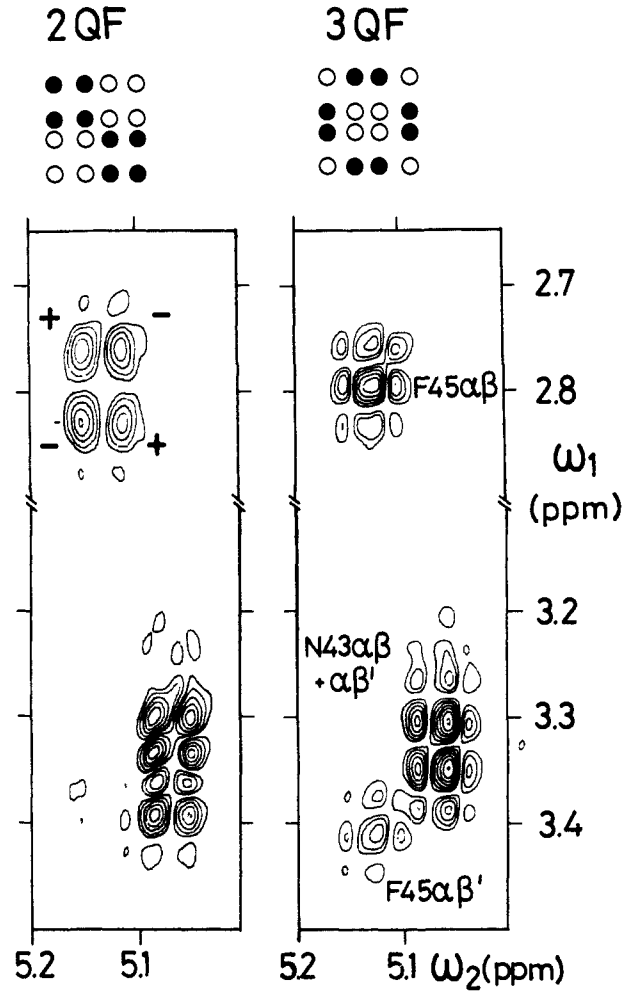

Figure 6. Effect of finite line width on 2QF-COSY and 3QF-COSY spectra. The schemes at the top represent multiplet patterns for $\alpha\beta$ cross-peaks without mutual overlap. Experimental $\alpha\beta$ cross-peaks of the $C^{\alpha}H$–$C^{\beta}H_2$ fragments in the amino acids Phe-45 and Asn-43 in BPTI clearly show the effects of overlap of two or several multiplet components.

We illustrate this by comparison of 2QF-COSY and 3QF-COSY cross-peaks in Figure 6. Whenever severe cancellation occurs for the four central multiplet components in 2QF-COSY, the same components interfere constructively in 3QF-COSY. If they become degenerate (e.g., in an AMX spin system with $J_{AM} = J_{AX} = J_{MX}$), the central region of the 3QF-COSY cross-peak experiences a fourfold increase in intensity compared to an individual multiplet component. This implies that in this limiting case the same effective sensitivity may be achieved for 3QF-COSY as for an ordinary COSY spectrum in the absence of overlap.

To quantify this effect for intermediate situations, we have simulated[21] A-M cross-peaks in 2QF-COSY and 3QF-COSY of an AMX spin system with $J_{Ax} = J_{MX}$ for different values of the ratio $(J_{AM} - J_{AX})$ to line width $\Delta_{1/2}$. In Figure 7 the intensity of the maximum peak height within the central four multiplet components is plotted vs. this ratio. Thereby we neglected overlap between the inner and outer lines of the cross-peaks, i.e., we assumed that each individual coupling constant exceeds the line width. As can be seen from the figure, the sensitivity in the region of the inner multiplet components of 3QF-COSY cross-peaks becomes superior to that of 2QF-COSY when the separation of the central lines decreases to a value below the line width. When the line width exceeds the separation of the central peaks by a factor of 1.4 or more, the central 3QF-COSY cross-peak com-

(19) Rance, M.; Sørensen, O. W.; Leupin, W.; Kogler, H.; Wüthrich, K.; Ernst, R. R. *J. Magn. Reson.* **1985**, *61*, 67–80.

(20) Boyd, J.; Dobson, C. M.; Porteus, R.; Redfield, C.; Soffe, N. Seventh International Meeting NMR Spectroscopy, Cambridge, 1985.

(21) The simulations were done with two spin-simulation programs. (a) Widmer, H.; Wüthrich, K. *J. Magn. Reson.*, in press. (b) Radloff, C.; Suter, D., unpublished.

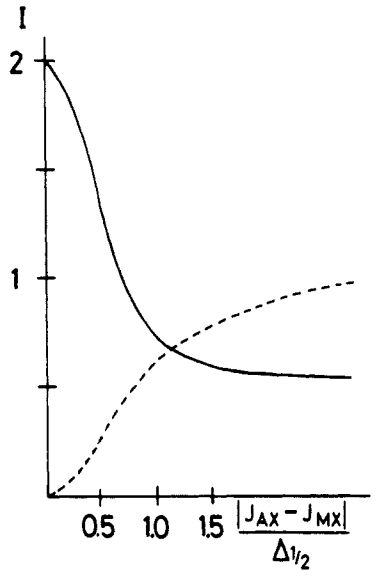

Figure 7. The maximum intensity I in the region of the four central multiplet components in the AM-cross-peak of an AMX spin system in 2QF-COSY (---) and 3QF-COSY (—) relative to an undisturbed multiplet component of the same line width is plotted vs. the ratio of peak separation $|J_{AM} - J_{AX}|$ to line width $\Delta_{1/2}$. In the computer simulations Lorentzian line shapes have been assumed. For simplicity, the coupling to the passive spins, J_{AX} and J_{MX}, have been assumed to be equal, and overlap with the outer multiplet components has been neglected.

ponents have actually a higher intensity than all multiplet components in the corresponding 2QF-COSY cross-peak.

The experimental spectra in Figure 6 clearly illustrate this fact. Taking into account the different scan numbers used for these particular spectra and neglecting overlap effects, in 3-spin systems the sensitivity of 3QF-COSY cross-peaks should be 61% of the 2QF-COSY cross-peaks. This ratio is met approximately by the outer multiplet components of the Phe-45 $\alpha\beta$ cross-peak (Figure 6). However, while the inner components in the 2QF cross-peak cancel completely, the amplitude of the inner components in the 3QF-COSY spectrum exceeds the amplitude of the corner components in the 2QF-COSY cross-peak by approximately 40%, as judged from the equidistant contour levels. This effect has even more pronounced consequences for the $\alpha\beta'$ cross-peak of Phe-45 in Figure 6. It can hardly be identified in the 2QF-COSY spectrum but is clearly visible in the 3QF-COSY spectrum. The opposite situation would occur when the coupling constant between the active spins is large and the couplings to the MQ-active spin are small. This would lead to constructive interference for the corner multiplet components in 2QF-COSY, while cancellation occurs in 3QF-COSY, as can be inferred from Figure 5.

The complementary behavior of even- and odd-quantum-filtered COSY spectra may serve not only to identify cross-peaks that are weak in 2QF-COSY due to cancellation effects but also to unravel complex, crowded spectral regions on the basis of the different symmetry properties of the cross-peaks. This is illustrated by Figure 4 showing parts of 2QF-COSY and 3QF-COSY spectra of the $\alpha\beta$ region for long side chain amino acids. The cancellation effects do not allow an unambigous identification of both $\alpha\beta$ cross-peaks of Glu-49, Arg-53, and Lys-26 in 2QF-COSY without relying on additional information from their $\beta\beta'$ cross-peaks. In contrast, the increase in sensitivity of the 3QF-COSY spectrum for the cross-peaks of Arg-53 and Glu-49 and the different symmetry of the multiplet patterns in 2QF-COSY and 3QF-COSY permit unambiguous identifications. Different cross-peak symmetries can also avoid mutual cancellation of multiplet components belonging to different, partially overlapping cross-peaks, as is exemplified by the two cross-peaks $\alpha\beta$ and $\alpha\beta'$ of Lys-26 in Figure 4.

6. Complications in Multiple-Quantum-Filtered COSY Spectra Encountered with Proteins

With the schemes of Figure 2 the selection rules for MQF-COSY provide us in principle with a straightforward guideline for simplifying the spectra of proteins and distinguishing between different ^1H spin systems. As mentioned earlier, these selection rules may break down in the presence of groups of equivalent spins or in systems with strong coupling, as is discussed in Sections 6.1 and 6.2. However, even in the absence of these more fundamental complications the MQF-COSY spectra are sometimes at variance with the expectations from the selection rules. In the following we give some indications of the kind of unexpected effects that one might encounter.

Comparison of 2QF-COSY, 3QF-COSY, and 4QF-COSY in Figure 8 reveals features which are immediately useful for spectral analysis and others which require further consideration. The positive aspects include that the reduction of the diagonal visible in the 3QF-COSY spectrum enables the identification of cross-peaks which are close to the diagonal and are not resolved in 2QF-COSY. This is exemplified by the Tyr-35 $\beta\beta'$ cross-peak. The 4QF-COSY spectrum does not exhibit unexpected peaks, and all visible cross-peaks belong to CH_2–CH_2 fragments. These occur exclusively in Glu, Gln, Met, Pro, Arg, and Lys, and thus 4QF-COSY facilitates the identification and delineation of long side chain spin systems. In Figure 8 this is illustrated by the correlations within the β and γ protons of Glu-49. These can hardly be unravelled in 2QF-COSY, whereas in 4QF-COSY the assignments are further supported by the characteristic antisym-

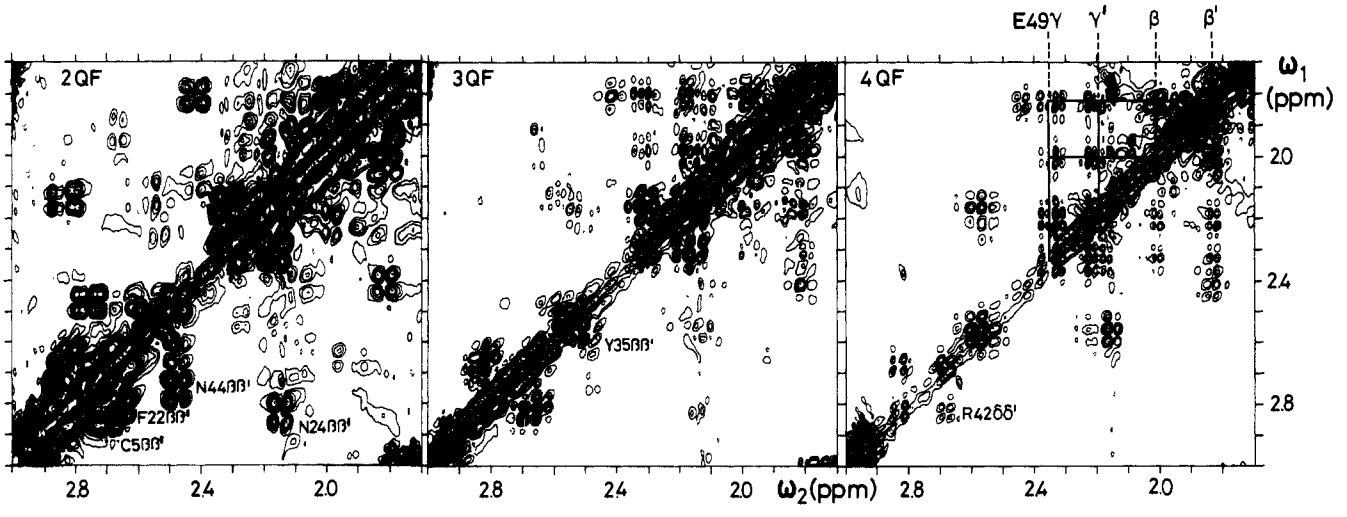

Figure 8. Geminal and vicinal cross-peaks of CH_2-fragments in 2QF-COSY, 3QF-COSY, and 4QF-COSY of BPTI. In 2QF-COSY and 3QF-COSY the $\beta\beta'$ cross-peaks of AMX spin systems are identified that are eliminated in 4QF-COSY. The connectivities between the side chain protons of Glu-49 and the $\delta\delta'$ cross-peak of Arg-42 are indicated in the 4QF-COSY spectrum.

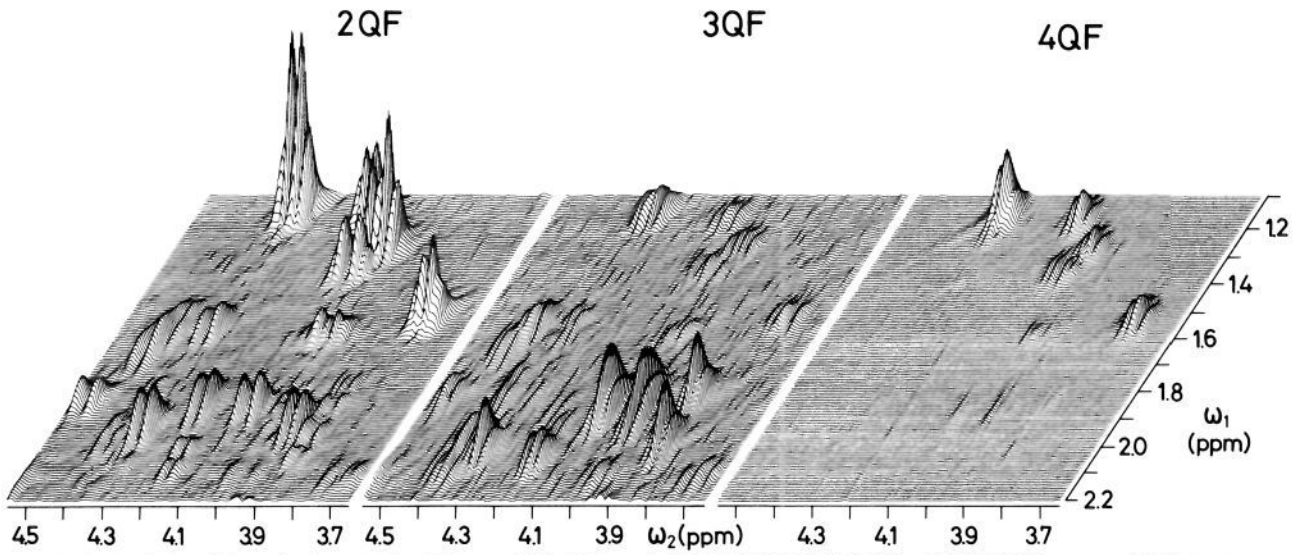

Figure 9. Stacked plots of the region (ω_1 = 1.10 – 2.20, ω_2 = 3.65 – 4.55 ppm) of 2QF-COSY, 3QF-COSY, and 4QF-COSY spectra of BPTI in absolute value display. 3QF-COSY contains "allowed" as well as "forbidden" cross-peaks, whereas only "forbidden" peaks are visible in 4QF-COSY. The "forbidden" peaks can be identified as Ala $\alpha\beta$ and Thr $\beta\gamma$ cross-peaks at the chemical shift coordinates [Ω_1/Ω_2(ppm)] 1.18/4.30 (Ala-16), 1.56/3.78 (Ala-25), 1.19/4.30 (Ala-27), 1.21/4.10 (Ala-40), 1.29/4.16 (Ala-58), 1.38/4.06 (Thr-11), and 1.59/4.00 (Thr-54). The intensity of the Ala cross-peaks exceeds that of all other cross-peaks in this 4QF-COSY spectrum by more than a factor of two.

metric sign pattern. The elimination of all 3-spin systems in 4QF-COSY allows one to localize also the Arg-42 $\delta\delta'$ cross-peak, which is hidden beneath the cross-peaks Cys-5 $\beta\beta'$ and Phe-22 $\beta\beta'$ in 2QF-COSY and 3QF-COSY.

Unexpected features in Figure 8 are that the $\beta\beta'$ cross-peaks of Asn-24 and Asn-44 are strongly attenuated in 3QF-COSY, even though none of these geminal cross-peaks should be removed by 3QF-COSY (Figure 2B). Similarily the $\beta\beta'$ cross-peaks of Cys-14, Cys-38, and Phe-4 are suppressed in the 3QF-COSY spectrum of Figure 3. This unexpected absence of particular cross-peaks in 3QF-COSY is probably due to disapperance of one or more couplings to the MQ-active spins. In proteins it is not uncommon that some couplings vanish for conformational reasons.

Overall, it would appear that the potential of MQF-COSY for unravelling complex ^{1}H NMR spectra of proteins can be largely realized in spite of these deviations from the predicted behavior (Figure 2). However, quite generally one must exercise care when drawing conclusions based on the *absence* of cross-peaks, and the situations to be discussed in the following two sections must be kept in mind when interpreting the *presence* of MQF-COSY peaks.

6.1. Amino Acid Residues Containing Methyl Groups. It is surprising that the $\alpha\beta$ and $\beta\gamma$ cross-peaks of the amino acids Ala and Thr, respectively, can be observed in the 3QF-COSY and 4QF-COSY spectra of Figure 9. According to the MQF selection rules of Section 2 these cross-peaks as well as the CH_3 diagonal peaks in AX_3 systems should be fully suppressed in 3QF-COSY or 4QF-COSY. Since the couplings between equivalent spins are ineffective, the AX_3 spin system possesses a star-like coupling network with A in the center. The X spins have effectively only a single coupling partner, and it should be impossible to convert X spin 1QC into 3QC or 4QC, and vice versa, which leads to the expected suppression of these peaks in 3QF-COSY or 4QF-COSY.[6]

It has recently been shown[10] that nonexponential relaxation of degenerate transitions[22] can explain the observed violations of the MQF selection rules. To grasp the basic idea it is sufficient to explain how 3QC can be generated in a CH_3 group starting from 1QC of the same group. For this purpose it is necessary to change the representation of the density matrix to the symmetry-adapted base. A system of three equivalent spins $I = {}^1/_2$ can be decomposed into the totally symmetric (A_1-type) states corresponding to a group spin $F = {}^3/_2$ and the states of E-type symmetry with a group spin $F = {}^1/_2$. For pQF-COSY spectra with $p > 2$, the response of the two-spin systems of E-type symmetry is fully suppressed. The density matrix σ_{F_x} representing 1QC of phase x for the group spin $F = {}^3/_2$ is given by[23]

$$\sigma_{F_x} = {}^1/_2 \begin{bmatrix} 0 & \sqrt{3} & 0 & 0 \\ \sqrt{3} & 0 & 2 & 0 \\ 0 & 2 & 0 & \sqrt{3} \\ 0 & 0 & \sqrt{3} & 0 \end{bmatrix} \quad (8)$$

When applying an rf pulse which causes a transformation of this matrix into a new matrix, σ', the contributions to the three-quantum elements σ'_{14} and σ'_{41} originating from the nonzero elements in eq 8 exactly cancel as long as the indicated relative amplitudes of $3^{1/2}/2$ apply. However, if a state with different relative amplitudes is created before applying the rf pulse with flip angle β, 3QC may be generated according to

$$\sigma'_{1,4} = (\sigma_{1,2} - 3^{1/2}\sigma_{2,3} + \sigma_{3,4})\sin^3\beta \quad (9)$$

Such a state can result from unequal relaxation of the three degenerate coherences in eq 8 in the course of the evolution period t_1 (see ref 11). This implies that more or less 3QC can be generated, depending on the efficiency and the mechanism of transverse relaxation. As a result, a 2QF-COSY or 3QF-COSY spectrum may exhibit a diagonal peak even for an isolated methyl group (this has indeed been observed for Met-52 in BPTI).

The situation is similar in the case of 4-quantum filtering of an AX_3 spin system. The nonexponential relaxation during t_1 leads normally to a superposition of two Lorentzian peaks of unequal widths and signs in 4QF-COSY. The "forbidden" diagonal peaks and cross-peaks have different flip angle dependencies for 3QF-COSY and 4QF-COSY. While the peaks are relatively weak for $\beta = \beta' = \pi/2$ in 3QF-COSY (generally weaker than the "allowed" cross-peaks, see Figure 9), they assume their maxima in 4QF-COSY for flip angles of $\pi/2$ (exceeding the "allowed" cross-peaks in amplitude).[11] Multiexponential relaxation causes noticeable sidelobes of the "forbidden" peaks in MQF-COSY, which might be misinterpreted as indicating additional fine structure.[10]

In Figure 2C the schematic MQF-COSY spectra of the methyl-bearing amino acids are compiled. We distinguish between cross-peaks (open circles) and diagonal peaks (filled circles) predicted by the MQF selection rules and the additional

(22) (a) Hubbard, P. S. *J. Chem. Phys.* **1969**, *51*, 1647–1651. (b) Hubbard, P. S. *J. Chem. Phys.* **1970**, *52*, 563–568. (c) Werbelow, L. G.; Marshall, A. G. *J. Magn. Reson.* **1973**, *11*, 299–313. (d) Werbelow, L. G.; Grant, D. M. *Adv. Magn. Reson.* **1977**, *9*, 190–299.

(23) Mehring, M. *High Resolution NMR in Solids*; Springer-Verlag: New York, 1983.

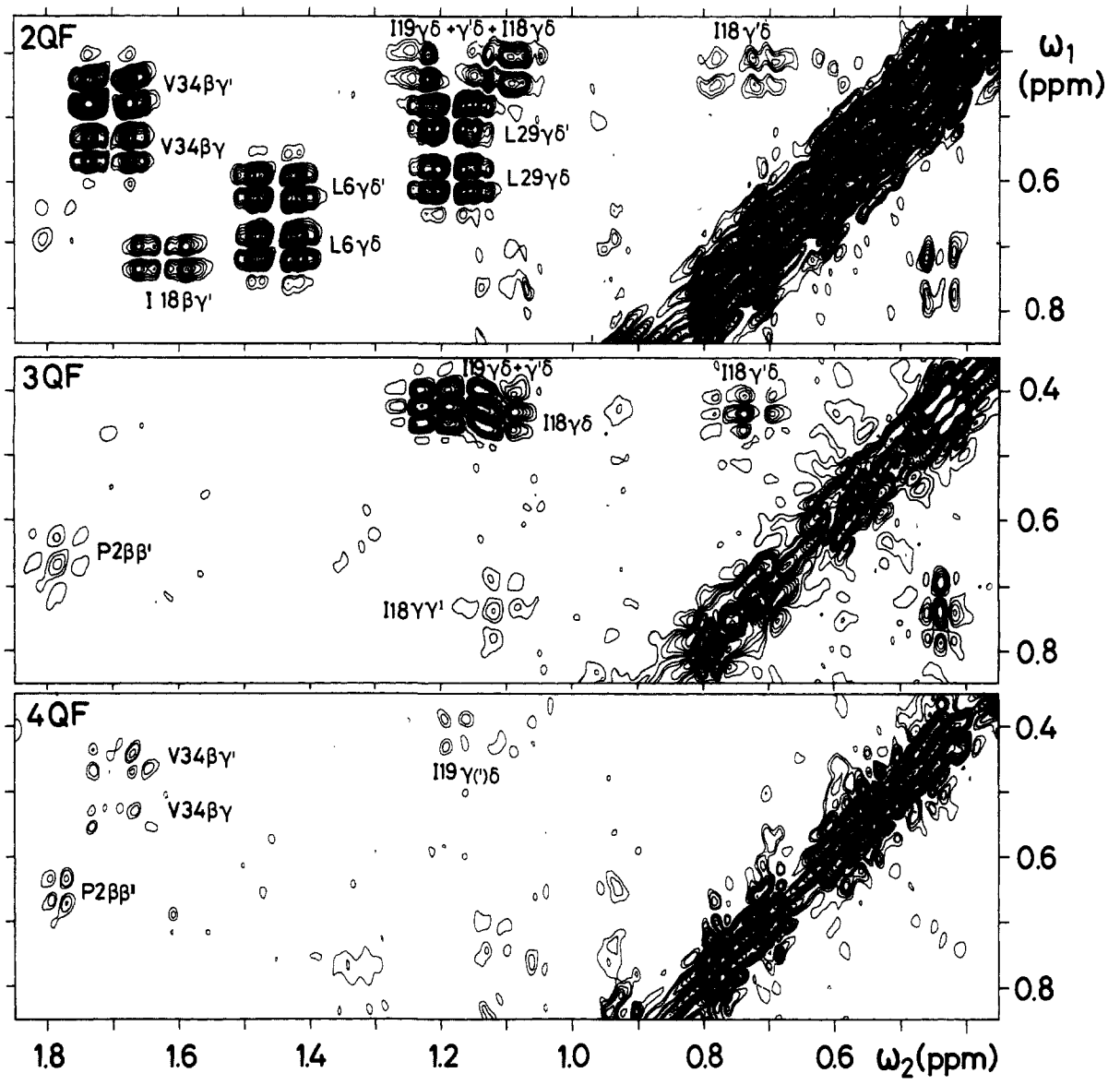

Figure 10. Aliphatic region of the 2QF-COSY, 3QF-COSY, and 4QF-COSY spectra of BPTI. The most intense cross-peaks are the CH_3 cross-peaks of Leu, Ile, and Val. Only the peaks that can unambiguously be assigned are identified by the usual symbols.

"forbidden" peaks introduced by multiexponential relaxation (asterisks). In *p*QF-COSY for $p > 3$, the only "allowed" cross-peaks are between geminal protons. "Forbidden" cross-peaks can be anticipated, however, for vicinal protons in filtered spectra with p up to 5 (see Ile in Figure 2C). There are also "forbidden" diagonal peaks appearing as a consequence of multiexponential relaxation in methyl groups.

The only "allowed" cross-peaks involving CH_3 groups in a *p*QF-COSY spectrum with $p > 2$ are the Ile-$\gamma\delta$ and Ile-$\gamma'\delta$ cross-peaks in 3QF-COSY (Figure 2C), originating from subsystems with three resolved mutual couplings. It turns out in practice that these peaks are stronger than the "forbidden" cross-peaks of other CH_3 groups in this spectral region, as is exemplified in Figure 10 by the partially overlapping $\gamma\delta$ and $\gamma'\delta$ cross-peaks of Ile-18 and Ile-19. 3QF-COSY can thus provide clear identification of the Ile-$\gamma\delta$ correlation.

When inspecting the aliphatic region in 2QF-COSY, 3QF-COSY, and 4QF-COSY of BPTI (Figure 10), no obvious "forbidden" cross-peaks can be detected in 3QF-COSY. In 4QF-COSY, weak responses from Val-34 $\beta\gamma$ are present, while the Leu-$\gamma\delta$ cross-peaks are suppressed. This can be rationalized in terms of the longer and more flexible side chain of Leu, where less pronounced nonexponential relaxation effects can be expected.

It can also be seen from Figure 2C that "allowed" diagonal peaks of protons coupled to methyl groups persist up to high orders of multiple-quantum filtering, in contrast to the cross-peaks which are all eliminated. If these resonances appear at characteristic

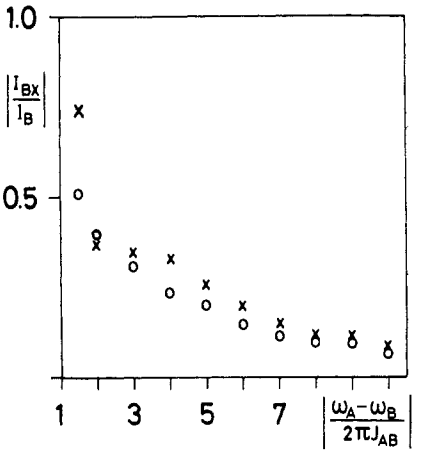

Figure 11. Intensity ratio $|I_{BX}/I_B|$ of the B-X cross-peak to the B diagonal peak in a 3QF-COSY spectrum of a linear ABX spin system as a function of $|(\Omega_A - \Omega_B)/2\pi J_{AB}|$ obtained by computer simulations for line widths of 1 Hz (×) and 10 Hz (○). The parameters used are given in the text.

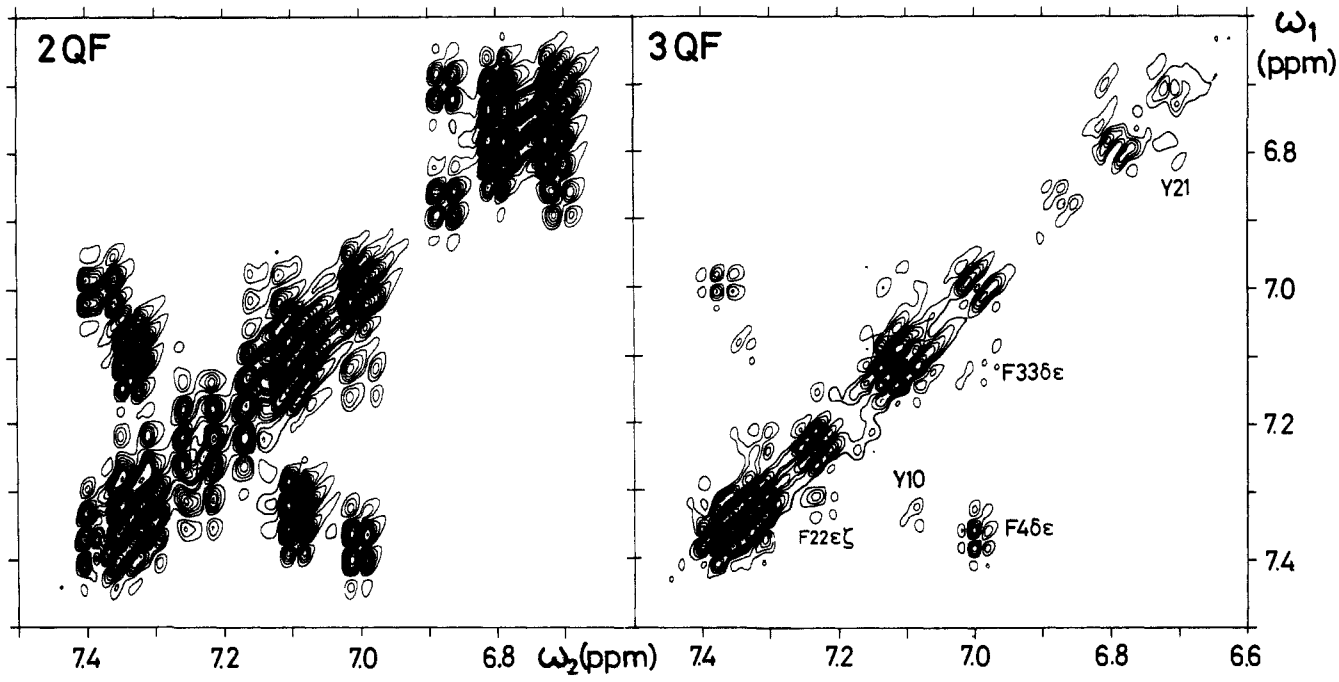

Figure 12. Part of the aromatic region of 2QF-COSY and 3QF-COSY spectra of BPTI. In the 3QF-COSY spectrum "forbidden" cross-peaks which arise from strong coupling between the aromatic ring protons are labeled by the usual symbols.

chemical shift positions, as for Thr-β, they may be used for the identification of amino acid resonances by one-dimensional MQF-spectra,[6a,24] as has recently been demonstrated by Rance et al.[9]

It should be noted that the "forbidden" peaks mentioned in this section show strong amplitudes only for molecules in the slow motion limit. Under conditions of extreme motional narrowing (that is in all small molecules) these peaks become vanishingly weak.[11]

6.2. Effects of Strong Coupling. Since in strongly coupled spin systems individual transitions can no longer be assigned to particular spins, a rf pulse can transfer coherence from any transition within a strongly coupled subsystem to a transition of a spin which is weakly coupled to any member of the strongly coupled subsystem and vice versa. This can lead to the appearance of additional cross-peaks, which are not expected on the basis of the MQF selection rules. In order to determine the conditions under which additional cross-peak multiplets in MQF-COSY spectra have measurable intensity for a linear ABX coupling network we have simulated[21] 3QF-COSY spectra assuming $J_{AX} = 0$, $J_{AB} = J_{BX} = 10$ Hz, $\Omega_X/2\pi = -1000$ Hz, $\Omega_B/2\pi = 0$ Hz, and varying $\Omega_A/2\pi$ from 15 to 500 Hz. In Figure 11 the absolute ratio of the peak height of the strongest multiplet component in the forbidden B-X cross-peak, I_{BX}, to the maximum peak height found in the allowed diagonal peak multiplet of spin B, I_B, (which is the only "allowed" peak in the 3QF-COSY spectrum) is plotted vs. the ratio $|(\Omega_A - \Omega_B)/2\pi J_{AB}|$. Under conditions of weak coupling, i.e., $\Omega_A/2\pi \geq 500$ Hz, only the diagonal peak of spin B is present. If $|(\Omega_A - \Omega_B)/2\pi J_{AB}|$ falls below a value of approximately 9, the intensity of the forbidden cross-peak exceeds 10% of the allowed diagonal peak in this spin system. (The 10% limit is considered to be a threshold for interpretable peaks in protein spectra). For the appearance of "forbidden" cross-peaks arising from strong coupling between two weakly coupled spins in pQF-COSY it is sufficient that *one* of these spins is strongly coupled to $(p - 2)$ additional spins, in contrast to the MQF selection rules for weak coupling (Section 2).

In BPTI additional cross-peaks arising from strong coupling effects were found in the aromatic region. In Figure 12 we compare partial 2QF-COSY and 3QF-COSY spectra of the aromatic ring protons. According to the MQF selection rules of Section 2 no cross-peaks should occur in the 3QF-COSY spectrum, as the coupling networks are essentially linear. (This takes into account that the broad lines disguise small couplings). By simulations we could show that the observed 3QF-COSY cross-peaks of Phe and Tyr can indeed be accounted for by strong coupling effects. The simulations showed that the most prominent cross-peak in Figure 12 (Phe-4 $\delta\epsilon$) is not caused by strong coupling between the δ and ϵ protons but by the even stronger coupling between the ϵ and ζ protons of the $\delta\delta'\epsilon\epsilon'\zeta$ spin system.

Complete analysis of strong coupling effects in MQF-COSY, however, requires more extensive simulations that will be presented at a later date.[21]

7. Technical Aspects of Multiple-Quantum-Filtered COSY

In this section we discuss the optimization of MQF-COSY experiments and indicate the parameters used for the experiments presented in this paper.

A first important aspect concerns the sensitivity of pQF-COSY to imperfect mixing pulses which may affect signal intensities and create artifacts. From the description of the coherence transfer process between evolution and detection in a MQF-COSY experiment in eq 6 it can be derived that the amplitude of the absorptive part of pQF-COSY cross-peaks varies with $\sin^{2p-2}(\beta)$, if we assume that both mixing pulses use equal flip angle β. With increasing order p of the MQF, the peak amplitudes become increasingly dependent on accurate values of β. In addition to the loss in signal amplitude, dispersive cross-peak components are created by deviations of the flip angles of the two pulses from $\pi/2$, with amplitudes proportional to $\sin^{2p-2}(\beta)\cos^2(\beta)$. To ease problems with pulse imperfections (e.g., due to inhomogeneous rf fields) it is advisable to use composite pulses as shown in Figure 1C, which has been employed for all the experiments shown here. More sophisticated compensation schemes[25] were also tested, but experience showed that there was no obvious advantage compared to the scheme of Figure 1C.

Noise trains parallel to the ω_1-axis, called t_1-*noise*, are common in 2D experiments and are due to instrumental instability.[26,27]

(24) Sørensen, O. W.; Levitt, M. H.; Ernst, R. R. *J. Magn. Reson.* **1983**, *55*, 104–113.

(25) Levitt, M. H. *Prog. Nucl. Magn. Reson. Spectrosc.*, in press.

(26) Mehlkopf, A. F.; Korbee, D.; Tiggleman, T. A. *J. Magn. Reson.* **1984**, *58*, 315–323.

(27) (a) Denk, W.; Wagner, G.; Rance, M.; Wüthrich, K. *J. Magn. Reson.* **1985**, *62*, 350–355. (b) Otting, G.; Widmer, H.; Wagner, G.; Wüthrich, K. *J. Magn. Reson.* **1986**, *66*, 187–193.

They tend to increase in amplitude in the long phase cycles needed for the higher order multiple quantum filters. It is often possible to reduce t_1-noise by reordering the sequence of phases within a phase cycle in such a way that scans using opposite phase are arranged in pairs. For example, instead of using the sequence $(0, \pi/3, 2\pi/3, 3\pi/3, 4\pi/3, 5\pi/3)$ for the excitation propagator of 3QF-COSY, the sequence $(0, 3\pi/3, \pi/3, 4\pi/3, 2\pi/3, 5\pi/3)$ is preferred. This scheme responds to a lesser extent to instrumental instabilities which have time constants exceeding the scan repetition time but are shorter than the duration of a complete phase cycle. We also found that the optimum sequencing of the phases may vary from spectrometer to spectrometer. An account of the possible sources of t_1-noise has recently been given by Mehlkopf et al.[26]

As the free induction decays (FID's) in MQF-COSY spectra are sine-modulated by the spin–spin coupling terms in both time dimensions (eq 6), all signal amplitudes for $t_1 = 0$ or $t_2 = 0$ should disappear. Nonzero amplitudes would give rise to offsets in the frequency domains known as t_1- and t_2-*ridges*.[27] It is therefore advisible not to acquire the FID for $t_1 = 0$ and instead use a set of zero data. Accordingly, the first point of each FID along t_2 (Figure 1) should be replaced by zero.

All spectra in this paper were recorded from the same sample of basic pancreatic trypsin inhibitor (BPTI, 20 mM in ^2H_2O, p^{2}H = 4.6, T = 36 °C) on a Bruker AM-360 spectrometer. By using the pulse sequence of Figure 1C with 8.4 μs $\pi/2$-pulses and a phase switching delay of 4 μs, 512 t_1-values were acquired with 2048 data points in the t_2-dimension. The spectral width was 3030.30 Hz in both dimensions. Axial peak suppression, alternation of the last pulse, and CYCLOPS[28] were performed in addition to the basic p-quantum filter phase cycling (eq 1). Overall this gave a number of 64 or 96 scans per t_1-value for 2QF-COSY or 3QF-COSY, respectively. The basic cycle was repeated twice for 4QF-COSY spectra, resulting in 256 scans per FID. The repetition interval was 1 s. Time proportional phase incrementation (TPPI) was used in conjunction with two-dimensional real cosine Fourier transformation to obtain pure phase spectra.[5d] Gauss–Lorentz window multiplication was applied in both dimensions (LB1 = −30, GB1 = 0.3, LB2 = −20, GB2 = 0.2) prior to zero filling to 4096 by 8192 data points and Fourier transformation. The same acquisition and processing parameters were used for all spectra shown in this paper, unless otherwise stated. Sets of contour plots for comparison of different pQF-COSY spectra were drawn with the same contour line levels. The first eight levels in each spectrum are equidistant, whereas higher levels have linearly increasing separation to allow for a high dynamic range. TSP served as internal chemical shift reference.

(28) Hoult, D. I.; Richards, R. E. *Proc. Roy. Soc. London, Ser. A* **1975**, *344*, 311–320.

8. Conclusions

Experience with higher order MQF-COSY showed that by comparing several MQF-COSY spectra, revealing insights can be obtained in cases where 2QF-COSY alone does not permit a full spectral analysis. In particular, the combination of 3QF-COSY and 4QF-COSY seems to be a promising approach.

The elimination of cross-peaks associated with a particular coupling network together with the characteristic symmetry of MQF-COSY cross-peak multiplets facilitates peak recognition in crowded spectral regions. In spectra with broad lines, constructive interference within cross-peak multiplets may increase the apparent sensitivity of 3QF-COSY cross-peaks above that of 2QF-COSY.

The MQF selection rules[6a] allow prediction of the spectral editing effected by MQF-COSY and form a basis for the identification of spin systems in MQF-COSY spectra. "Forbidden" cross-peaks not predicted by the MQF selection rules may be caused by multiexponential relaxation in methyl groups or by strong coupling. This apparent complication can be exploited for peak assignments, as long as one keeps in mind the basic facts pointed out in Section 6 to prevent misinterpretations.

MQF-COSY experiments of a higher order than those presented here have inherently low sensitivity and require powerful instrumentation to become practically feasible. Overall, MQF-COSY experiments present a valuable supplement to the arsenal of 2D NMR methods for the investigation of biological macromolecules and are expected to find their main application under circumstances where the traditional methods like 2QF-COSY or relayed coherence transfer spectroscopy leave ambiguities.

Acknowledgment. We are grateful to Dr. G. Bodenhausen, Dr. O. W. Sørensen, and Dr. G. Wagner for stimulating discussions and to C. Radloff and H. Widmer for performing part of the computer simulations with their programs. Financial support provided by the Kommision zur Förderung wissenschaftlicher Forschung (project 1329) and by Spectrospin AG, Fällanden, is gratefully acknowledged.

Registry No. BPTI, 9087-70-1; L-Cys, 52-90-4; L-Ser, 56-45-1; L-Ash, 70-47-3; L-His, 71-00-1; L-Phe, 63-91-2; L-Tyr, 60-18-4; L-Trp, 73-22-3; Gly, 56-40-6; L-Arg, 74-79-3; L-Pro, 147-85-3; L-Ile, 73-32-5; L-Met, 63-68-3; L-Lys, 56-87-1; L-Val, 72-18-4; L-Glu, 56-86-0.